Available online at www.sciencedirect.com
ScienceDirect
Applied Catalysis B: Environmental 79 (2008) 394–401
APPLIED CATALYSIS B: ENVIRONMENTAL
www.elsevier.com/locate/apcatb

Preparation of Au/TiO_2 catalysts from Au(I)–thiosulfate complex and study of their photocatalytic activity for the degradation of methyl orange

Baozhu Tian, Jinlong Zhang *, Tianzhong Tong, Feng Chen

Laboratory for Advanced Materials and Institute of Fine Chemicals, East China University of Science and Technology, 130 Meilong Road, Shanghai 200237, PR China

Received 16 July 2007; received in revised form 1 November 2007; accepted 3 November 2007
Available online 12 November 2007

Abstract

Gold loaded on TiO_2 (Au/TiO_2) catalysts were prepared using Au(I)–thiosulfate complex ($Au(S_2O_3)_2^{3-}$) as the gold precursor for the first time. The samples were characterized by UV–vis diffuse reflectance spectra, X-ray diffraction (XRD), transmission electron microscopy (TEM), atomic absorption flame emission spectroscopy (AAS), and X-ray photoelectron spectroscopy (XPS) methods. Using $Au(S_2O_3)_2^{3-}$ as gold precursor, ultra-fine gold nanoparticles with a highly disperse state can be successfully formed on the surface of TiO_2. The diameter of Au nanoparticles increases from 1.8 to 3.0 nm with increasing the nominal Au loading from 1% to 8%. The photocatalytic activity of Au/TiO_2 catalysts was evaluated from the analysis of the photodegradation of methyl orange (MO). With the similar Au loading, the catalysts prepared with $Au(S_2O_3)_2^{3-}$ precursor exhibit higher photocatalytic activity for methyl orange degradation when compared with the Au/TiO_2 catalysts prepared with the methods of deposition–precipitation (DP) and impregnation (IMP). The preparation method has decisive influences on the morphology, size and number of Au nanoparticles loaded on the surface of TiO_2 and further affects the photocatalytic activity of the obtained catalysts.

Keywords: Au/TiO_2; Photocatalytic activity; Degradation; $Au(S_2O_3)_2^{3-}$; Au loading

1. Introduction

Bulk Au has long been regarded as a highly inert metal with little or no chemical and catalytic activity [1,2]. However, Haruta et al. found that Au can exhibit surprisingly high catalytic reactivity when it is highly dispersed on selective metal oxides (Au/oxides) [3–5]. Up to now, Au/oxide catalysts have become one of the hottest systems in catalysis, being widely applied to many important processes, such as CO oxidation, selective oxidation of propene, nitrogen oxide reduction, and photocatalytic oxidations used for environmental cleanup [4,6–8]. It has been confirmed by various studies that the catalytic property of Au/oxide catalysts depends significantly on the size of Au particles, the interaction between Au and the supporting oxide, as well as the nanostructure of the active sites [4,9,10]. For the purpose of obtaining structures which can facilitate high performance catalysis, many chemical and physical methods, such as co-precipitation [9], chemical vapor deposition (CVD) [11], co-sputtering [12], deposition–precipitation (DP) [13,14] and gas-phase grafting (GG), [11,15] have been developed.

Amongst the wet-chemical methods, the conventional impregnation (IMP) method, which is unlikely to deposit highly dispersed Au nanoparticles on the surface of oxides, has been reported to be incompetent for preparing highly active Au/oxide catalysts. In contrast, the DP has been demonstrated to be one of the most successful methods for depositing highly dispersed Au nanoparticles because it allows the size of the gold particles to be adjusted by controlling the pH of the preparation and the calcination temperature. In this method, the gold precursor, typically chloroauric acid ($HAuCl_4$), is dissolved in solution and deposited on the surface of support in the form of $Au(OH)_3$ by adjusting the pH of $HAuCl_4$ aqueous solution to a fixed pH values (pH 6–10). DP is an effective method for depositing highly dispersed Au nanoparticles on the surface of MgO, TiO_2, and Al_2O_3, the isoelectric points of which are above 5. Since gold hydroxide cannot be deposited at low pH, this method is not suitable for metal oxides having low points of zero charge, for example, SiO_2 (IEP = 2), SiO_2–Al_2O_3 (IEP = 1) and WO_3 (IEP = 1) [6,16]. Although it is possible to prepare Au/oxides

* Corresponding author. Tel.: +86 21 64252062; fax: +86 21 64252062.
E-mail address: jlzhang@ecust.edu.cn (J. Zhang).

0926-3373/$ – see front matter © 2007 Elsevier B.V. All rights reserved.
doi:10.1016/j.apcatb.2007.11.001

under acidic condition via the anion adsorption of Au precursor, low Au loading is always unavoidable after the samples being washed [17]. So, it is a significant work of exploring new methods for depositing highly dispersed Au nanoparticles on the surface of metal oxides under acidic condition. Furthermore, it is economically favorable of using low Au loading for Au/oxide catalysts because the price of gold is very expensive. Another purpose of this study is to investigate whether it is possible to obtain Au/oxide catalysts with highly catalytic activity under the condition of low gold loading.

In the preparation of silver halide photographic emulsions, chemical sensitization are often carried out by adding chemical sensitizer into the emulsion to form chemical sensitization centers, which are effective for forming latent image. $Au(S_2O_3)_2^{3-}$ was considered to be a good sensitizer for the formation of chemical sensitization centers. It was found that formation of $Au(S_2O_3)_2^{3-}$ results in enhancement of both the incorporation of Au^+ into silver halide grains and formation of sulfide ions on the grain surface to give sulfur-plus gold sensitization centers composed of both silver sulfide and gold sulfide during digestion of emulsions with chloroauric acid and sodium thiosulfate [18]. Enlightened by this chemical sensitization method, $Au(S_2O_3)_2^{3-}$ complex was selected as a gold precursor to prepare Au/TiO_2 catalysts in this work. Although it is difficult for Au^+ to enter the crystal lattice of TiO_2 because the ionic radius of Au^+ is much bigger than that of Ti^{4+}, it is possible to form gold sulfide on the surface of TiO_2 under acidic condition. The gold sulfide will further decompose after calcination treatment, resulting in the formation of metallic Au. The photodegradation of MO dye was chosen as a probe reaction to measure the photocatalytic activity of Au/TiO_2 catalysts. For comparison, Au/TiO_2 samples were also prepared with DP and IMP method, respectively.

2. Experimental section

2.1. Preparation of Au/TiO_2 catalysts

Degussa P25 (TiO_2) was used as support ($45\ m^2\ g^{-1}$, nanoporous, 70% anatase and 30% rutile, purity > 99.5%) and was dried beforehand in air at 100 °C for 24 h. All of the following preparations were performed in the absence of light, which is known to decompose and reduce Au precursors.

For the preparation of Au/TiO_2, $Au(S_2O_3)_2^{3-}$ aqueous solution was beforehand prepared by slowly adding $HAuCl_4$ aqueous solution to excess $Na_2S_2O_3$ aqueous solution under magnetic stirring (the mole ratio of $HAuCl_4$ to $Na_2S_2O_3$ was 1:4.3). At first, the pH value of 60 mL of $Au(S_2O_3)_2^{3-}$ aqueous solutions was adjusted to 2 with diluted hydrochloric acid (1 M). Subsequently, 1 g of TiO_2 (P25) was added to this solution, followed by ultrasound irradiation in an ultrasonic cleaning bath (Elma, T660/H, 35 kHZ, 360 W) at 80 °C for 4 h. Then, the precipitate was separated from the precursor solution by centrifugation, and washed with distilled water four times to remove residual Cl^- and Na^+ ions, as well as, Au species not interacting with the support. Finally, the sample was dried under vacuum at 100 °C for 2 h, heated from room temperature to a certain temperature with a heating rate of 2 °C/min, and calcined at this temperature for 4 h. The obtained samples were labeled as S_x-T, in which the "x" refers to the nominal mass percentage content of Au in the Au and TiO_2, and "T" refers heat-treating temperature in centigrade degree. By similar post-treating processes mentioned above, Au/TiO_2 catalysts were also prepared with impregnation and DP (NaOH, pH 8.0) methods, and designated as IMP_x-T and DP_x-T, respectively.

2.2. Characterization

X-Ray diffraction (XRD) measurements were carried out with a Rigaku D/max 2550 VB/PC X-ray diffractometer at room temperature using Cu Kα radiation (λ = 0.154056 nm) and a graphite monochromator, operated at 40 kV and 100 mA. UV–vis diffuse reflectance spectra (DRS) were obtained using a Scan UV–vis–NIR spectrophotometer (Varian Cary 500) equipped with an integrating sphere assembly, using polytetrafluoroethylence (PTFE) as a reference material. The state of Au on the surface of TiO_2 was observed with a JEOL JEM-100 CX II transmission electron microscopy (TEM), operated at an acceleration voltage of 100 kV. The X-ray photoelectron spectroscopy (XPS) measurements were carried out on a PerkinElmer PHI 5000C ESCA X-ray photoelectron spectrometer with Al Kα radiation at 250 W. The binding energies were corrected for the surface charge by referencing to C 1s peak of contaminant carbon at 285 eV. The content of Au in Au/TiO_2 samples was determined by atomic absorption flame emission spectroscopy (AAS) (Shimadzu AA-6400F). The Au loading of the samples is expressed in grams of Au per gram of sample: $\text{wt\% Au} = m_{Au}/(m_{Au} + m_{TiO_2}) \times 100$.

2.3. Photocatalytic activity measurement

The photocatalytic activity of the Au/TiO_2 samples was measured in terms of the degradation of methyl orange (MO, Scheme 1). The photodegradation reactions were carried out with a homemade photoreactor, in which a 300 W high-pressure Hg lamp (λ_{max} = 365 nm) was used. The lamp was cooled with flowing water in a quartz cylindrical jacket around the lamp, and ambient temperature is maintained during the photodegradation reaction because of good ventilation. The distance between the light and the reaction tube was fixed at 24 cm. For each measurement, 0.05 g of photocatalyst sample was added into a 70 mL quartz tube containing 50 mL of 30 mg/L MO. Before photoreaction, the mixture was sonicated for 10 min and stirred in the dark for 30 min to attain the adsorption–desorption equilibrium for MO and dissolved oxygen on the surface of TiO_2. At every given time interval, a sample of 3.5 mL suspension was withdrawn, centrifuged and filtered. The absorbance of the residual MO in the solution was measured with a UV–vis spectrophotometer (Varian Cary 100) at 464 nm, which is the

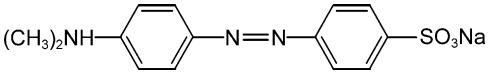

Scheme 1. Molecular structure of methyl orange.

maximum absorption of MO. The degradation rate of MO was calculated from the determined absorbance.

3. Results and discussion

3.1. UV-vis diffuse reflectance spectra

Fig. 1 shows the UV–vis diffuse reflectance spectra of sample S_4-*T* calcined at different temperatures. Compared with untreated P25, there is a red-shift of absorption edge for P25 experienced washing and drying treatment. For the untreated P25, the absorption edge is around 400 nm, which is between the absorption edge of anatase (387 nm) and rutile (418 nm). This can be ascribed to that P25 consists of anatase and rutile. The reason why washing and drying treatment can result in red-shift of the adsorption edge of P25 is still puzzled and further investigation is under way. In the case of samples S_4-*T*, an absorbance band around 545 nm arises and the intensity of the absorbance band increases with increasing the calcination temperature from 200 to 350 °C. According to the relevant references [19–22], the absorbance band should be ascribed to the plasmon resonance of metallic Au particles. For metal nanoparticles of Au^0, Cu^0, and Ag^0, the plasmon absorption arises from the collective oscillations of the free conduction band electrons that are induced by the incident electromagnetic radiation. For Au/TiO_2 samples, the intensity of absorbance band is related to the size of Au particles and the content of Au in Au/TiO_2. There is only a slight increase of the absorbance intensity when the calcination temperature of sample S_4-*T* increases from 300 to 350 °C, suggesting that the size of Au has no evident increase and gold exists in the state of metallic gold.

3.2. X-ray diffraction

The XRD patterns of P25, S_8-300, S_8-400, and S_8-500 are shown in Fig. 2a–d, respectively. As shown in Fig. 2, the shapes and intensities of the diffraction peaks for both anatase and rutile in the four samples are very similar, indicating that calcining at 300 or 500 °C for 4 h did not change the content and particle size of anatase and rutile in the samples. By careful observation, it can be found that new peaks emerge at $2\theta = 38.2$, 44.4, 64.6 and 77.6°, which can be attributed to the diffraction peaks of (1 1 1), (2 0 0), (2 2 0) and (3 1 1) planes of polycrystalline Au, respectively (overlap occurred between the (1 1 1) diffraction peak of Au and the (1 0 1) diffraction peak of rutile). The above-mentioned results confirmed the formation of metallic gold. The diffraction peaks of Au become more intense and narrow with increasing the heat-treating temperature from 300 to 500 °C, suggesting the increase of the average size of the Au nanoparticles. Haruta and co-workers [23] also reported that the particle size of Au was increased with increasing calcination temperature. At $2\theta = 77.6°$, the diffraction peak of Au shows no overlap with those of anatase and rutile. The average crystallite size of Au can be calculated by applying the Debye–Scherrer formula [24],

$$D = \frac{K\lambda}{\beta \cos\theta}$$

where *D* is the average crystallite size, *K* is a constant which is taken as 0.89 here, λ is the wavelength of the X-ray radiation (Cu Kα = 0.154056 nm), β is the corrected band broadening (full width at half-maximum (FWHM)) after subtraction of equipment broadening, and θ is the diffraction angle. The average crystallite sizes of samples S_8-400 and S_8-500 were calculated to be 9.0 and 12.4 nm, respectively. Compared with samples of S_8-400 and S_8-500, the diffraction peak of sample S_8-300 was broader and lower, suggesting a smaller average crystallite size of Au for the sample S_8-300 (cannot be calculated because of very low peak intensity).

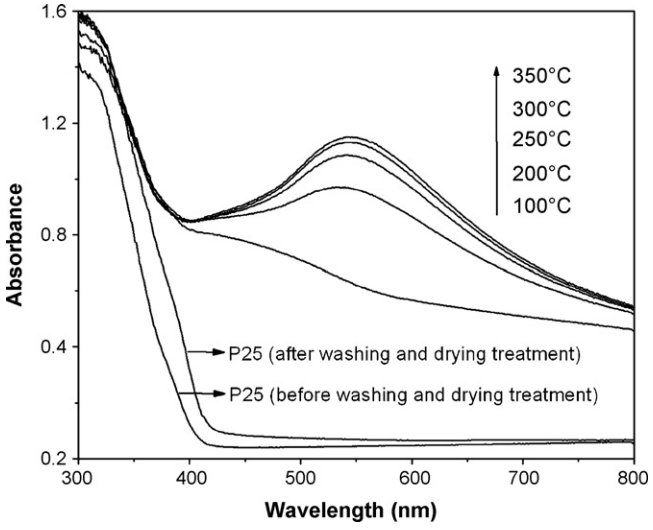

Fig. 1. UV–vis DRS of sample S_4 as a function of different calcination temperatures.

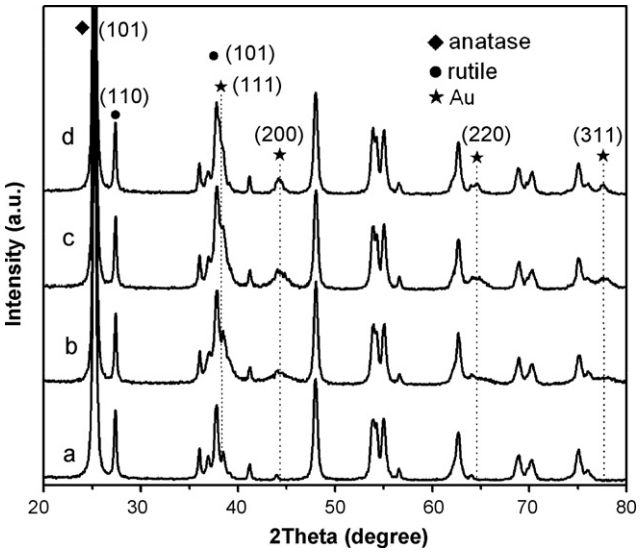

Fig. 2. XRD patterns of (a) P25, (b) S_8-300, (c) S_8-400 and (d) S_8-500.

3.3. AAS and TEM analysis

The actual Au loadings of different samples were examined by AAS analysis and were shown in Table 1.

Table 1
Au loading (wt%) of Au/TiO_2 samples

Nominal Au loading (wt%)	Au loading (wt%)[a]		
	IMP_x	DP_x	S_x
0.1	0.09	0.10	0.09
1	0.82	1.01	0.95
4	1.15	3.61	3.54
8	3.12	6.21	7.38

[a] Determined by AAS.

For the samples prepared with IMP method, the Au loading percentage decreases with increasing the nominal Au loading. This phenomenon might be related to the pH value variation of $HAuCl_4$ solution. At high $HAuCl_4$ concentration, the pH value is low and the main Au species in solution exist in the form of $AuCl_4^-$, which can electrostatically interact with the TiO_2 surface [17]. Due to the low adsorption forces between the $AuCl_4^-$ ions and TiO_2 surface, part of the Au should be washed out, resulting in low Au loading percentage. In our experiment, it seems very hard to acquire an actual gold loading higher than 3.5% when the sample after washing whatever the initial Au loading. With the decrease of $HAuCl_4$ concentration, the pH value of $HAuCl_4$ solution gradually increases and Au species in solution exist in the form of $Au(OH)Cl_3^-$, adsorbed on the TiO_2 surface via forming surface complex by reaction with surface OH^- (Eq. (1)) [17], leading to the increase of Au loading percentage.

$$TiOH + Au(OH)Cl_3^- \leftrightarrow TiOAuCl_2 + H_2O + Cl^- \quad (1)$$

In the case of DP method, Au gold species in solution exist in the form of $Au(OH)_3Cl^-$ and form hydroxide deposition on the specific sites of TiO_2, resulting in high Au loading percentage [17]. The reason why $Au(S_2O_3)_2^{3-}$ precursor method favors the improvement of Au loading percentage will discuss hereafter.

TEM analysis was carried out to observe the morphology and size of the Au particles dispersed on the surface of TiO_2. Fig. 3 shows the TEM images and Au particle size distributions of Au/

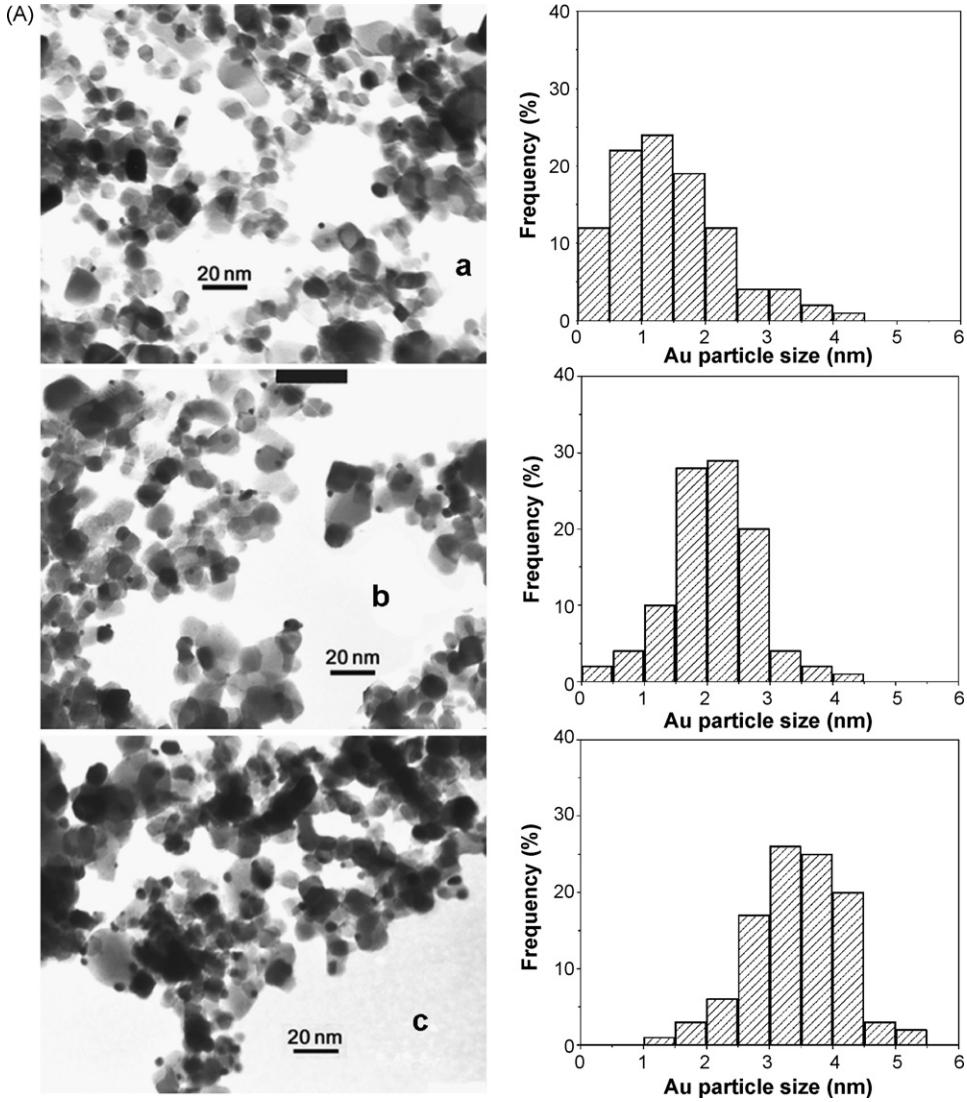

Fig. 3. TEM images and Au particle size distributions of Au/TiO_2 samples prepared by DP (A: a–c) and $Au(S_2O_3)_2^{3-}$ precursor method (B: d–f): (a) DP_1-300; (b) DP_4-300; (c) DP_8-300; (d) S_1-300; (e) S_4-300 and (f) S_8-300.

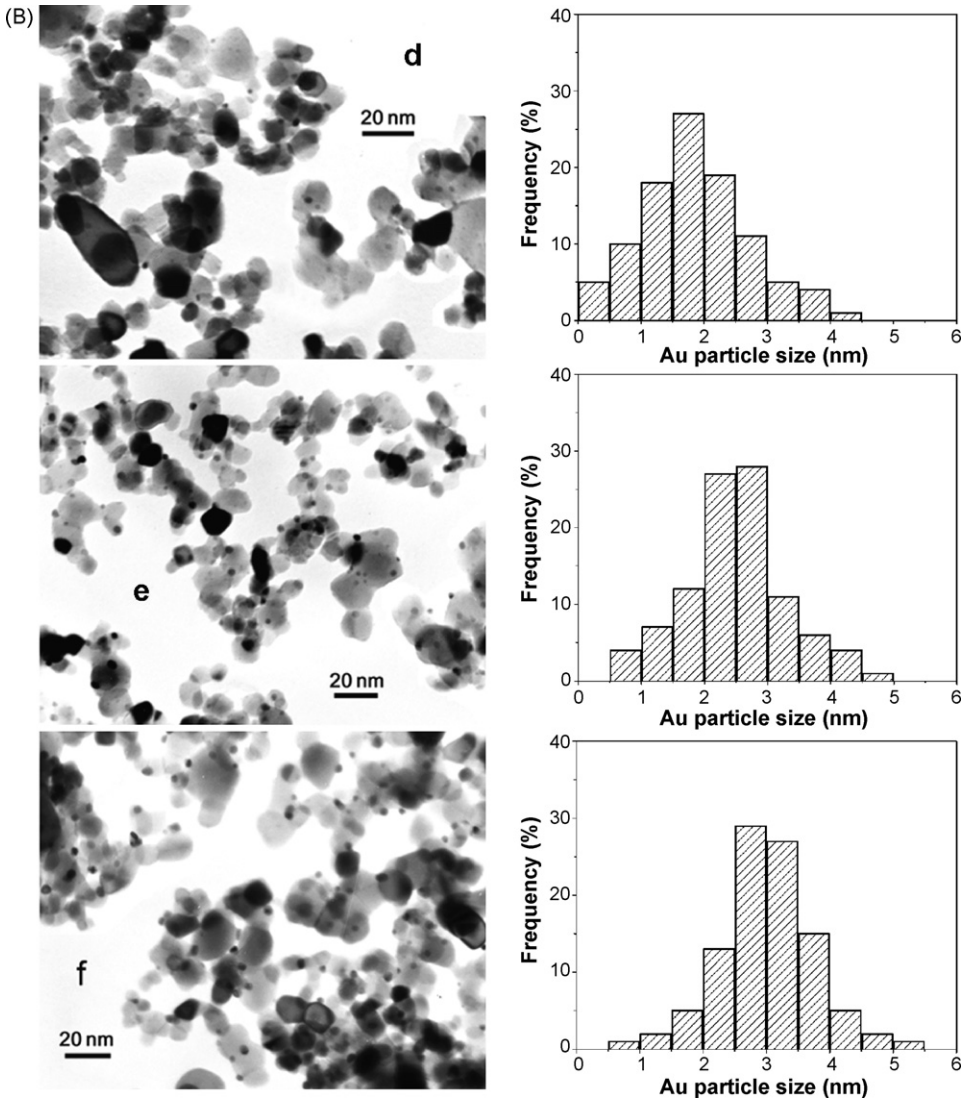

Fig. 3. (*Continued*).

TiO_2 samples prepared by DP (Fig. 3A: a–c) and $Au(S_2O_3)_2^{3-}$ precursor method (Fig. 3B: d–f). The spherical Au nanoparticles dispersed on the surface of TiO_2 particles were observed as dark spots having obvious contrast with the support. Within a certain series (DP or S), the mean diameter of Au particles has a gradually increase with the increase of Au loading, e.g., ~1.8 nm for S_1-300, ~2.5 nm for S_4-300, and ~3.0 nm for S_8-300, together with the increase of the number of Au particles on the surface of TiO_2. However, this situation is not suitable for the different series. For instance, the actual Au loadings for samples IMP_8-300, DP_4-300 and S_4-300 are similar (Table 1), but the number of Au nanoparticles on sample S_4-300 is more than that of sample DP_4-300, and only a few Au particles (3–8 nm) were found on the surface of sample IMP_8-300 (TEM image was not shown). Based on the fact that the actual gold loading of sample IMP_8-300 is much higher than that of sample S_1-300, less number of dispersed gold nanoparticles was formed on sample IMP_8-300 than on sample S_1-300, it is reasonable to think that most Au loaded on the samples prepared with IMP method exists in the form of "gold coating", which cannot be clearly observed by TEM because of the low contrast between the "gold coating" and the TiO_2 support. TEM results indicate that the existent state of Au loaded on the surface of TiO_2 is closely related to the preparation methods.

3.4. XPS analysis

XPS analysis was performed to elucidate the chemical oxidation state of Au nanoparticles loaded on TiO_2. Fig. 4a, b displays the XPS Au 4f spectra of samples S_4-100 and S_4-300, respectively. As shown in Fig. 4b, the doublet peaks located at 83.3 and 86.8 eV can be assigned to the characteristic doublets of Au° loaded on TiO_2 [25], suggesting that only elemental Au is formed on the TiO_2 surface. According to the XPS hand books and the previous reports [26,27], the double peaks for bulk metallic Au were centered at 84.0 and 87.7 eV, respectively. The shift of Au 4f peaks of Au/TiO_2 toward lower binding energies can be due to the negative charge of the

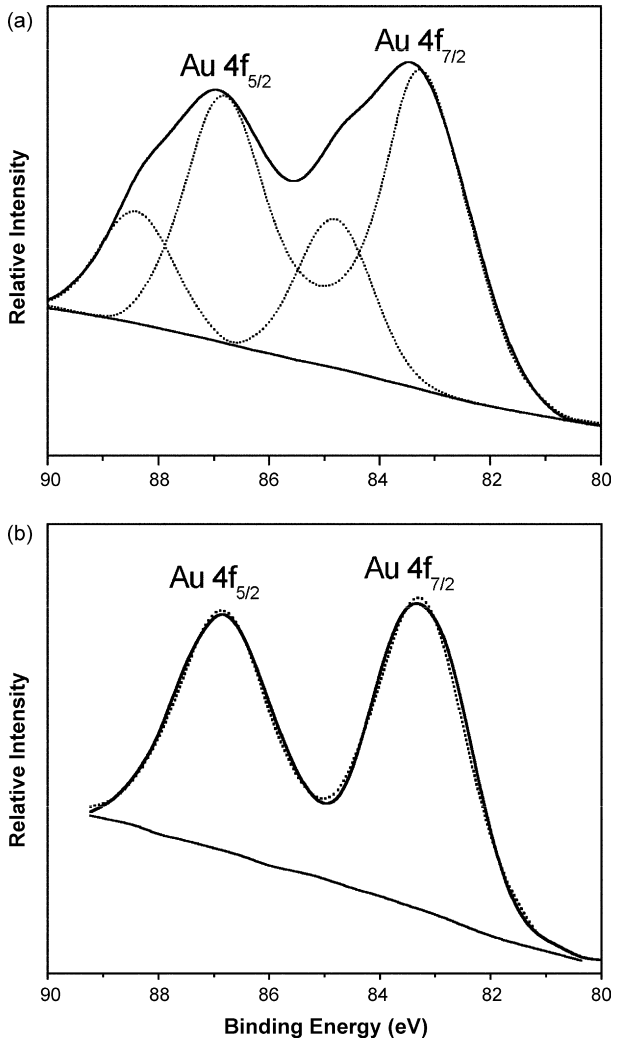

Fig. 4. XPS Au 4f spectra of (a) S_4-100 and (b) S_4-300.

Au nanoparticles because of the charge transfer from the TiO_2 substrate. Negative charge of the Au nanoparticles can be understood because of the large difference in the workfunction of Au and TiO_2. Thus, electron transfer is facilitated from TiO_2 to Au [28]. For sample S_4-100 (Fig. 4a), the Au 4f doublet peaks appeared to be broad and evident asymmetrical, suggesting the presence of different Au species. The deconvoluted Au 4f peaks indicate that two components coexist in Au $4f_{7/2}$ and Au $4f_{5/2}$ signals, giving peaks at 83.3 and 84.8 eV for Au $4f_{7/2}$ signal as well as 86.8 and 88.4 eV for Au $4f_{5/2}$ signals. The two components can be attributed to metallic Au° and non-metallic Au (Au^{+}), respectively [29–31]. In addition, the presence of sulfur element was also confirmed by XPS analysis. Unfortunately, the chemical valence of sulfur cannot be judged because of the irregular shape and low intensity of S 2p peak.

Although $Au(S_2O_3)_2^{3-}$ can steadily exist under alkaline and excess $S_2O_3^{2-}$ conditions, it might gradually decompose with increasing temperature under acidic condition, resulting in the formation of Au sulfide (Au_2S) adsorbed on the surface of TiO_2. Due to the insolubility of Au sulfide in aqueous solution, high Au loading percentage can be easily realized. According to the relational references [32], gold sulfide (Au_2S) would decompose at 240 °C and form metallic gold. Therefore, it can be confirmed that gold species should exist in the form of metallic gold after the catalysts calcined at 300 °C for 4 h. The XRD and DRS results are also consistent with above-mentioned presumption.

3.5. Photocatalytic activity

The photocatalytic activity of S_x-300 serial catalysts, together with IMP_x-300 and DP_x-300 series for comparison, were determined by the photodegradation of MO aqueous solution. MO is a photostable dye and cannot be photodegraded in the absence of any catalyst under UV or visible light irradiation. Moreover, no further degradation of MO except initial adsorption on the surface of the samples was observed in the dark. As is well known, the photodegradation rate of MO is relative to pH value of reaction solution. But in our experiments, all the solutions for photocatalytic reaction were in weak acid condition and no evident change of pH was found. The constancy of pH value may ascribe to two reasons. Firstly, the catalyst samples after washing and calcining treatment become near neutral. Furthermore, the amino-containing products derived from dimethyl amino- and azo-groups (see Scheme 1), might neutralize the generated hydrosulfate ions and thus stabilize the pH value.

As mentioned above, washing and drying treatment can result in red-shift of the adsorption edge of P25, but it hardly changes the catalytic activity of P25 under UV light irradiation. Thus, untreated P25 was used as a reference photocatalyst in the photodegradation experiments. Fig. 5 illustrates the degradation percentage of MO with various Au/TiO_2 catalysts under UV light irradiation for 20 min. For each of nominal Au loadings, 0.1, 1, 4, and 8 wt%, the photocalytic activity of these samples varies in a descending order: S_x-300 > DP_x-300 > IMP_x-300 > P25. It was found that the photocatalytic activity depends more on the preparation method rather than the Au loading. For instance, Sample S_1-300, its actual Au loading

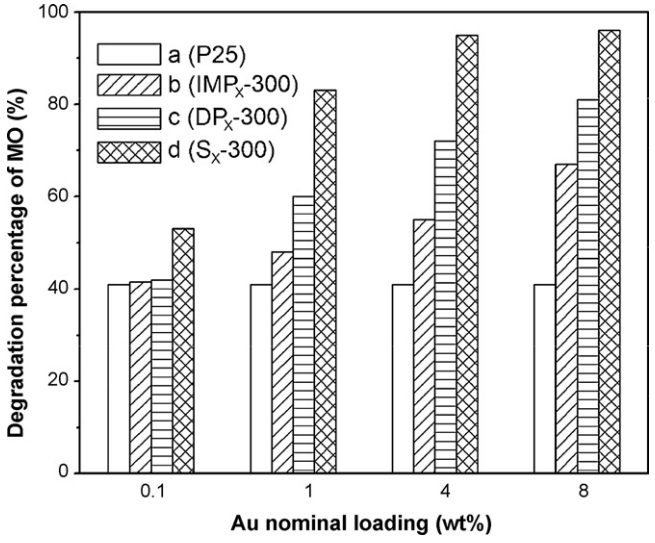

Fig. 5. Photodegredation of methyl orange with various Au/TiO_2 catalysts under UV light irradiation for 20 min: (a) P25; (b) IMP_x series; (c) DP_x series and (d) S_x series.

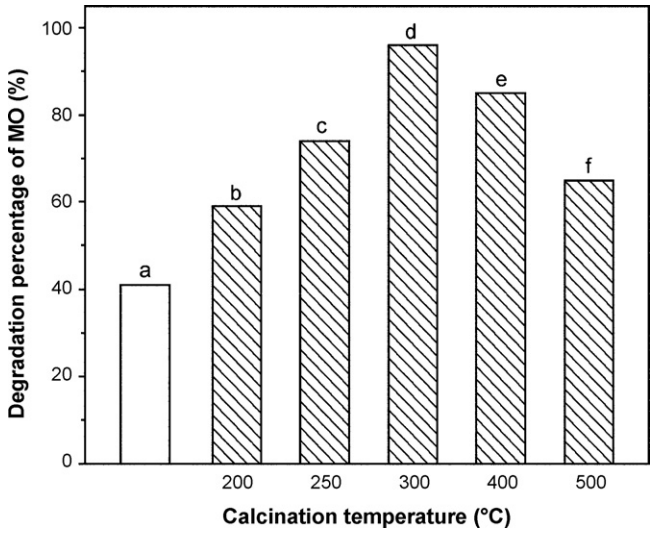

Fig. 6. Photodegredation of MO with S_8-*T* serial catalysts under UV irradiation for 20 min. (a) P25; (b) S_8-200; (c) S_8-250; (d) S_8-300; (e) S_8-400 and (f) S_8-500.

is 0.95%, exhibits higher photocatalytic activity than samples IMP_8-300 and DP_8-300, whose actual Au loadings were 3.12% and 6.21%, respectively. It is worth mentioning that using the $Au(S_2O_3)_2^{3-}$ precursor, an Au loading of 0.1 wt% (sample $S_{0.1}$-300) can evidently improve the photocatalytic activity of TiO_2 catalyst, whereas, a similar Au loading using IMP (sample $IMP_{0.1}$-300) or DP (sample $DP_{0.1}$-300) method can hardly improve the photocatalytic activity of TiO_2 catalysts. It is well known that low loading is economically favorable.

Fig. 6 shows the degredation of MO with S_8-*T* serial catalysts under UV irradiation for 20 min. As shown in Fig. 6, the photocatalytic activity of the samples S_8-*T* increases with increasing calcination temperature at the beginning, and has a downtrend with optimum photocatalytic activity at the calcination temperature of 300 °C. Combined the results that the crystalline size of Au particles increases with the increase of the calcination temperature (in Fig. 2), it is reasonable to consider that an appropriate diameter are essential for the acquisition of highly photocatalytic activity.

Fig. 7 shows the energy levels of valence band and conduction band of TiO_2, gold particles, and adsorbed O_2 on the TiO_2 surface, which can determine the direction of electronic flow [33–35]. As shown in Fig. 7, the electrons cannot directly or

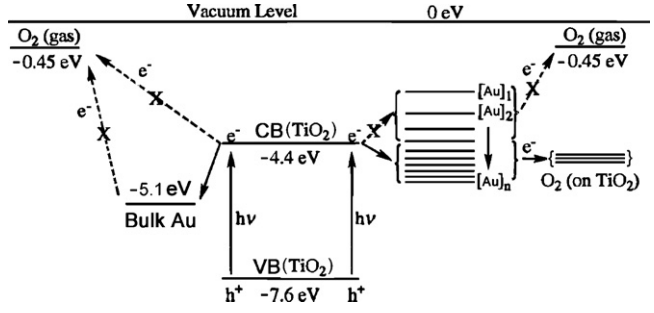

Fig. 7. Electronic energy level of gold particles, valence band and conduction band of TiO_2 and adsorbed O_2.

indirectly flow from bulk gold to adsorbed O_2 because the energy level of adsorbed O_2 is higher than that of bulk gold. So, bulk Au cannot increase the photocatalytic activity of TiO_2. Based on the fact that the Fermi energy of metal particles increases with decreasing size, because of quantum size effect, the Au particles with an appropriate size can possess an energy level between the conduct band of TiO_2 and the adsorbed O_2. Thus, the photoelectrons can be captured by gold particles and subsequently be transferred to the adsorbed O_2, leading to the effective separation of electrons and holes, and consequently increasing the photocatalytic activity of TiO_2. When the size of gold particles is too large, the Fermi energy of gold particles will be lower than that of adsorbed O_2 and the photoelectrons cannot be transferred to adsorbed O_2. Whereas the size of Au particles is too small, photoelectrons also cannot be transferred from the bottom of TiO_2 conduction band to the gold particles because the Fermi energy of gold particles is higher than that of adsorbed TiO_2 conduction band. Therefore, Au particles with an appropriate size are effective for the improvement of photocatalytic activity. In the above-mentioned experiments, the method of $Au(S_2O_3)_2^{3-}$ precursor favors the formation of Au particles with an appropriate size. Thus, the catalysts prepared with this method can show high photocatalytic activity for MO degradation. For the IMP_x serial samples, the "Au coating" with appropriate size is also favorable for the improvement of photocatalytic activity. The number of "Au coating" with appropriate size increases with increasing the nominal Au loading form 1% to 8%, thus, the photocatalytic activity also increases following the same order. However, it is noteworthy that "Au coating" seems to be low effective for the improvement of photocatalytic activity when compared with "dispersed Au particle".

4. Conclusions

Au/TiO_2 catalysts were prepared using $Au(S_2O_3)_2^{3-}$ as the gold precursor for the first time. The diameter of Au nanoparticles can be tuned in a certain range by adjusting the nominal Au loading and the calcination temperature. Compared with the Au/TiO_2 catalysts prepared with the methods of impregnation and deposition–precipitation, the catalysts prepared with $Au(S_2O_3)_2^{3-}$ precursor exhibit higher photocatalytic activity even if under low Au loading, perhaps ascribing to the formation of Au nanopaticles with appropriate size and number. Prepared with $Au(S_2O_3)_2^{3-}$ precursor, high Au loading percentage was easily obtained, which is beneficial to sparing the amount of Au used. More importantly, this method has prospects for loading Au nanoparticles on the acidic metal oxides like SiO_2 and WO_3, while deposition–precipitation is usually not valid to these metal oxides.

Acknowledgements

This work has been supported by Program for New Century Excellent Talents in University (NCET-04-0414); Shanghai Nanotechnology Promotion Centre (0552nm019, 0752nm001), National Nature Science Foundation of China (2057709, 20773039), the National Basic Research Program of China

(2004CB719502, 2007CB613306) and the Ministry of Science and Technology of China (2006AA06Z379, 2006DFA52710). A part of research work was finished in Shanghai Nanotechnology Joint Lab.

References

[1] G.C. Bond, D.T. Thompson, Catal. Rev. Sci. Eng. 41 (1999) 319.
[2] B. Hammer, J.K. Norskov, Nature 376 (1995) 238.
[3] M. Haruta, M. Daté, Appl. Catal. A 222 (2001) 427.
[4] M. Haruta, Catal. Today 36 (1997) 153.
[5] M. Valden, X. Lai, D.W. Goodman, Science 281 (1998) 1647.
[6] M. Haruta, Cattech 6 (2002) 102.
[7] G.C. Bond, D.T. Thompson, Gold Bull. 33 (2000) 41.
[8] J.A. Rodriguez, G. Liu, T. Jirsak, J. Hrbek, Z.P. Chang, J. Dvorak, A. Maiti, J. Am. Chem. Soc. 124 (2002) 5242.
[9] M. Haruta, N. Yamada, T. Kobayashi, S. Iijima, J. Catal. 115 (1989) 301.
[10] T. Tabakova, V. Idakiev, D. Andreeva, I. Mitov, Appl. Catal. A 202 (2000) 91.
[11] M. Okumura, K. Tanaka, A. Ueda, M. Haruta, Solid State Ionics 95 (1997) 143.
[12] T. Kobayashi, M. Haruta, S. Tsubota, H. Sano, Sens. Actuators, B 1 (1990) 222.
[13] S. Tsubota, M. Haruta, T. Kobayashi, A. Ueda, Y. Nakahara, Stud. Surf. Sci. Catal. 63 (1991) 695.
[14] M. Haruta, S. Tsubota, T. Kobayashi, H. Kageyama, M.J. Genet, B. Delmon, J. Catal. 144 (1993) 175.
[15] M. Okumura, S. Tsubota, M. Iwamoto, M. Haruta, Chem. Lett. (1998) 315.
[16] M. Haruta, Catal. Surveys Jpn. 1 (1997) 61.
[17] R. Zanella, S. Giorgio, C.R. Henry, C. Louis, J. Phys. Chem. B 106 (2002) 7634.
[18] T. Tani, Photographic Sensitivity: Theory and Mechanisms, Oxford University Press, New York, 1995, pp. 164–183.
[19] X.Z. Li, F.B. Li, Environ. Sci. Technol. 35 (2001) 2381.
[20] S.Y. Zhao, S.H. Chen, S.Y. Wang, Z.L. Quan, J. Colloid Interf. Sci. 221 (2000) 161.
[21] R. Zanella, S. Giorgio, C.H. Shin, C.R. Henry, C. Louis, J. Catal. 222 (2004) 357.
[22] I.M. Arabatzis, T. Stergiopoulos, D. Andreeva, S. Kitova, S.G. Neophytides, P. Falaras, J. Catal. 220 (2003) 127.
[23] S. Tsubota, D.A.H. Cunningham, Y. Bando, M. Haruta, Preparation of Catalysts, vol. VI, Elsevier, Amsterdam, 1995, p. 227.
[24] J. Lin, Y. Lin, P. Liu, M.J. Meziani, L.F. Allard, Y.P. Sun, J. Am. Chem. Soc. 124 (2002) 11514.
[25] T.L. Barr, S. Seal, J. Vac. Sci. Technol. A 13 (1995) 1239.
[26] Y.C. Liu, L.J. Juang, Langmuir 20 (2004) 6951.
[27] M.C. Henry, C.C. Hsueh, B.P. Timko, M.S. Freund, J. Electrochem. Soc. 148 (2001) D155.
[28] T. Ioannides, X.E. Verykios, J. Catal. 161 (1996) 560.
[29] S. Minicò, S. Scirè, C. Crisafulli, S. Galvagno, Appl. Catal. B 34 (2001) 277.
[30] Y. Yuan, K. Asakura, A.P. Kozlova, H. Wan, K. Tsai, Y. Iwasawa, Catal. Today 44 (1998) 333.
[31] T.M. Salama, T. Shido, H. Minagawa, M. Ichikawa, J. Catal. 152 (1995) 322.
[32] Y.Y. Lu, W.D. Bing, The Metallurgy of Noble Metals, Central South University Press, Changsha, 2002, pp. 8–12.
[33] T. Sakata, Heterogeneous photocatalysis at liquid–solid interfaces, in: N. Serpone, E. Pelizzetti (Eds.), Photocatalysis: Fundamentals and Applications, Wiley, New York, 1989, p. 311.
[34] S. Altunata, K.L. Cunningham, M. Canagaratna, R. Thom, R.W. Field, J. Phys. Chem. A 106 (2002) 1122.
[35] M. Sadeghi, W. Liu, T.-G. Zhang, P. Stavropoulos, B. Levy, J. Phys. Chem. 100 (1996) 19466.